ELSEVIER

Journal of Structural Geology 30 (2008) 444–450

JOURNAL OF STRUCTURAL GEOLOGY

www.elsevier.com/locate/jsg

The ''isogon rosette'' method for rapid estimation of strain in flattened folds

Deepak C. Srivastava*, Jyoti Shah

Department of Earth Sciences, IIT Roorkee, Roorkee 247667, India

Received 23 June 2007; received in revised form 30 January 2008; accepted 31 January 2008
Available online 8 February 2008

Abstract

Dip isogons, drawn on the profile section of a fold by linking the points of equal dip on the inner and outer arcs, can be arranged in a rosette by displacing the isogons without changing their orientation until the mid-point of each isogon becomes the common point of intersection of all isogons. The end points of isogons in the rosette trace a characteristic curve that defines the fold geometry. This curve is a circle in parallel folds, an ellipse in flattened parallel folds, and it reduces to a pair of points in ''similar'' folds. Since isogons deform as material lines during flattening, the characteristic curve, namely, the ellipse, directly represents the strain ellipse in flattened parallel folds. The method is tested successfully on several examples of natural flattened parallel folds. The ''isogon rosette'' method allows representation of a given fold by a point on the R_s–θ plot, where R_s and θ are the two-dimensional strain ratio and the angle between the maximum principal strain and the fold axial trace, respectively.

Keywords: Parallel fold; Isogon; Flattening; Strain; Fold classification

1. Introduction

Structural geologists have long used the shapes of folds for determining the amount of shortening due to folding in layered rocks (de Sitter, 1958; Ramsay, 1962; Ramsay, 1967, pp. 411–415; Ramsay, 1974). Amongst a large variety of natural fold shapes, the flattened parallel folds are most ideally suited for estimation of strain that is accommodated during the later, flattening phase of a fold's history. The profile sections of such folds are characterized by a greater curvature of the inner arc compared to that of the outer arc, and a greater thickness of layering in the hinge zone compared to that in the fold limbs (Fig. 1).

Buckling is a well known mechanism for the development of parallel folds in a competent layer enclosed in an incompetent medium of sufficient viscosity contrast (Ramberg, 1961; Ramsay, 1967, p. 386; Hudleston, 1973a). Flattening, i.e., a homogeneous strain superimposed on a parallel, or Class 1B fold, modifies its geometry into a flattened parallel or a Class 1C fold (Ramsay, 1967, p. 411). Estimates of flattening strain in Class 1C folds allow restoration of parallel fold shapes that in turn can be used to decipher the amount of shortening due to buckling. The estimate of buckle shortening, in turn, allows restoration of original length and thickness of undistorted beds, provided the layer-parallel shortening during the initial stages of folding is insignificant. Such restorations are of use to sedimentologists, structural geologists, petroleum geologists and stratigraphers.

2. Existing methods

The t'_α–α method and the ϕ–α method have been used most extensively for strain determination in Class 1C folds (Ramsay, 1967, p. 413; Hudleston, 1973b; Naha and Halyburton, 1977). The two methods are based on variations in the normalized layer thickness t'_α, and the angle between the isogon and normal to the tangents ϕ, with respect to the limb dip angle α at different points on a folded layer. These conventional methods, however, entail a large number of linear and/or

* Corresponding author. Tel.: +91 1332 285558; fax: +91 1332 273560.
E-mail address: dpkesfes@iitr.ernet.in (D.C. Srivastava).

0191-8141/$ - see front matter © 2008 Elsevier Ltd. All rights reserved.
doi:10.1016/j.jsg.2008.01.010

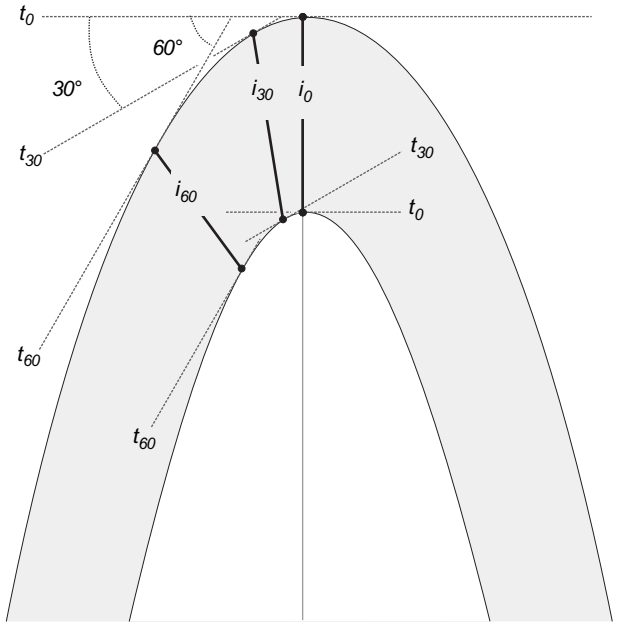

Fig. 1. Profile section of a flattened parallel (Class 1C) fold. The dip isogons i_0, i_{30} and i_{60}, are respectively obtained by joining the points at which the lines t_0, t_{30} and t_{60} are tangents on the outer and the inner arcs of the fold.

angular measurements and matching of plots of these measurements with sets of standard curves.

As the $t'_\alpha - \alpha$ and the $\phi - \alpha$ plots represent the variation of relative thickness of different portions of a fold limb by a curved line, these methods are not very useful for graphical representation of a large number of folds. Furthermore, the methods are best suited to those Class 1C folds that are flattened, such that the angle θ between the axial trace of the fold and the maximum principal strain direction is 0°. This condition is, however, not met in many natural folds since oblique flattening of folds is common in ductile shear zones and transpressive regimes (Srivastava and Srivastava, 1988). Although the inverse-thickness method (Lisle, 1992), the Mohr circle method and the Wellman method (Wellman, 1962; Shah and Srivastava, 2006) provide the strain estimates irrespective of the oblique nature of flattening, they too require a large number of linear and angular measurements, and/or geometrical constructions.

The dip isogons are the lines joining the points of equal dip on the outer arc and the inner arc of a folded layer (Fig. 1). In this article, we first give a new method that is based on arranging the dip isogons into a rosette which can then be used for strain estimation in flattened folds. We then extend the scope of the method by devising a unified scheme of fold classification and by suggesting a simple two-dimensional plot for representing each fold as a single data point.

3. The "isogon rosette" method

The method is based on two principles: (i) all dip isogons in a Class 1B fold are of equal length, and (ii) the isogons behave as material lines during flattening. Consider the profile section of a Class 1B fold with a few dip isogons drawn at different angles of limb dip (Fig. 2a). If we displace the isogons without changing their respective orientations, and arrange them so that they all intersect at the mid-point of each isogon (Fig. 2a), we produce a rosette in which the end points of the isogons trace a characteristic curve. The curve for a Class 1B fold is a circle with its centre located at the common point of intersection of isogons and a diameter equal to the common length of the isogons (circle below fold in Fig. 2a).

If we now flatten the Class 1B fold into a Class 1C fold by superimposing a homogenous strain, such that the angle θ between the major axis of the strain ellipse and the fold axial trace is 0°, the isogons experience changes in length and orientation. The circle, circumscribing the isogon rosette of the original Class 1B fold (Fig. 2a), transforms into an ellipse that circumscribes the isogon rosette of the Class 1C fold (Fig. 2b). The axial ratio and orientation of the ellipse records the two-dimensional strain ratio R_s and the principal strain orientation in terms of angle θ. With increasing amounts of flattening, the variably oriented dip isogons increasingly rotate into parallelism with the maximum principal strain direction. Eventually, at very high strains, the Class 1B fold modifies to a near "similar" or Class 2 fold, where all isogons become equal in length and lie approximately parallel to the axial trace. The characteristic curve defined by the end points of the isogon rosette reduces to a pair of points in the Class 2 folds (Fig. 2c).

The superimposition of homogeneous strain at an angle θ equal to 90° modifies a parallel, or Class 1B, fold into a Class 1A fold (Fig. 2d). If the superimposition of homogeneous strain onto the parallel fold is obliquely inclined to the fold axial trace, i.e., $0° < \theta < 90°$, then the parallel fold is modified into an obliquely flattened parallel fold, which may conform to the geometry of the Class 1C, or Class 1A fold, depending upon whether θ is close to 0° or 90°, respectively (Fig. 2e). On the down-plunge profile views, the obliquely flattened parallel folds can be further classified into Class +1C and Class −1C, or Class +1A and Class −1A folds, depending upon whether the maximum principal strain is shifted anticlockwise or clockwise relative to the fold axial trace (Fig. 2e). In summary, the strain ellipse representing the flattening suffered by folds is directly given by the ellipse that circumscribes the isogon rosette in all Class 1C and Class 1A folds, irrespective of the value of the angle θ.

The shape of the characteristic curve passing through the end points of the isogons in the rosette can also be used to restore the pre-flattened fold shape using widely available computer graphics software (Srivastava and Shah, 2006). The procedure involves the following three steps: (i) import the image of the flattened fold, together with the isogon rosette and the characteristic elliptical curve (Fig. 3a); (ii) group and rotate these objects until the major axis (x) of the ellipse becomes vertical (Fig. 3b); and (iii) stretch the objects by dragging the handle *4* in Fig. 3b to the right until the ellipse becomes a circle (Fig. 3c). This restores the shape of pre-flattened fold, which in this example is a parallel fold (Fig. 3c).

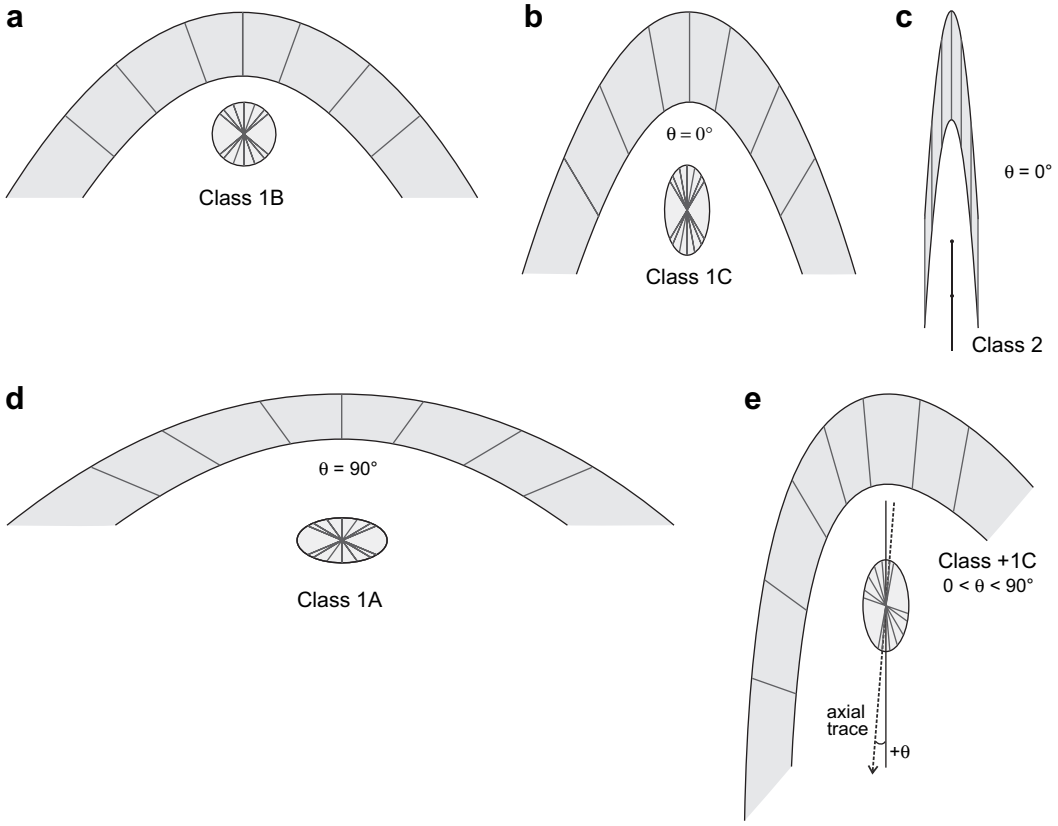

Fig. 2. (a–e) Profile sections with isogons in different classes of folds. The characteristic curves passing through the end points of the isogon rosettes are shown below each fold. The angle θ gives the obliquity between the fold axial trace and the maximum principal strain. Note that obliquely flattened Class 1A folds can develop for a range of θ values.

4. Examples

Hudleston (1973a) distinguishes three types of Class 1C folds to illustrate the scope and the limitations of the t'_α–α and the ϕ–α methods. The tangents at the hinge points of the outer and inner arcs are parallel in the Type 1 and Type 2 folds, whereas the two tangents are non-parallel in Type 3 folds. A Class 1C fold is classified as Type 1, or Type 2, depending upon whether or not the tangents are orthogonal to the fold axial trace, respectively.

To test the validity of the ''isogon rosette'' method, we have estimated the superimposed flattening strains for a large

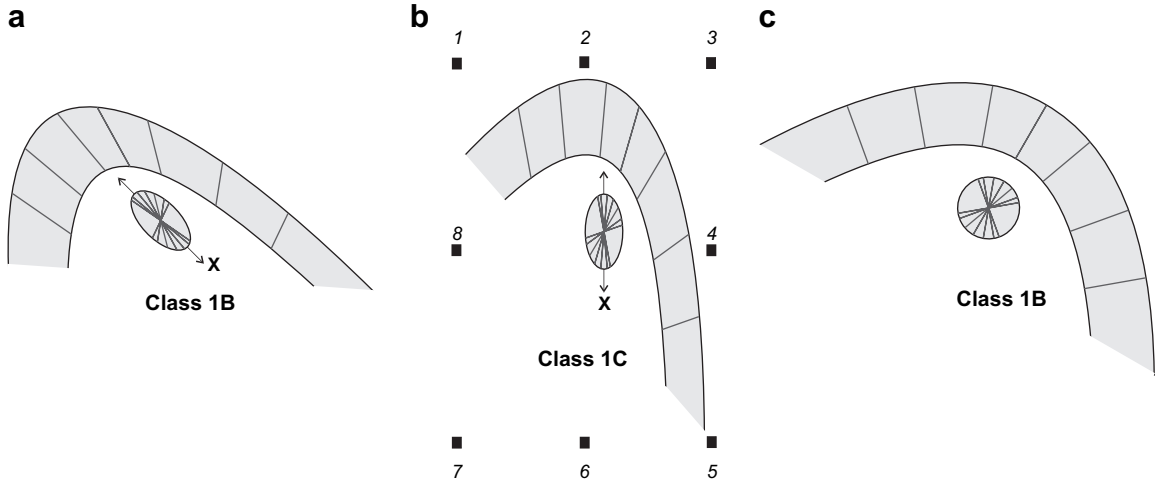

Fig. 3. Restoration of the pre-flattened fold shape. (a) image of the flattened parallel fold along with the isogon rosette and the circumscribing ellipse. x is the major axis of the ellipse. (b) Rotation of the objects in (a) such that the x direction becomes vertical. *1–8* are dragging handles. (c) Restored fold shape obtained by stretching the handle *4* in (b) to the right until the ellipse transforms into a circle.

number of published and unpublished images of the three different types of Class 1C folds; we have compared these results to those obtained using the $t'_\alpha - \alpha$ and the $\phi - \alpha$ methods (Fig. 4, Table 1). Type 1 folds yield consistent results using all three methods. Type 2 folds cannot be analysed using the $t'_\alpha - \alpha$ method, and the application of the $\phi - \alpha$ method on these folds is tedious and prone to error. No estimate of strain can be made using the $t'_\alpha - \alpha$ or the $\phi - \alpha$ method in Type 3 folds. By contrast, the "isogon rosette" method efficiently determines strain in all three types of Class 1C folds (Table 1).

5. Flattening in Class 3 folds

The estimation of flattening strain for Class 3 folds is based on the assumption that the buckling of a multilayer sequence, consisting of an incompetent layer sandwiched between two competent layers, produces a Class 3B fold in the incompetent layer. The existing definition of a Class 3B fold (Zagorčev, 1993) requires its association with a Class 1B fold, such that the layer thicknesses along the axial trace of the Class 1B and the Class 3B folds are same. Based on this definition, we give a simple geometrical criterion for classification of Class 3 folds.

Consider a Class 3 fold with h_1 and h_2 as the hinge points located on the inner and the outer arcs, respectively (Fig. 5a). While keeping the outer arc fixed, move the inner arc upwards along the axial trace until the hinge point h_1 shifts to the point h_3, such that $h_1h_2 = h_2h_3$ (Fig. 5b). This interchange of the outer and inner arcs transforms the Class 3 fold into a Class 1 fold (Fig. 5b). If the geometries of the transformed folds are Class 1A, 1B or 1C this implies that the original Class 3 fold is a Class 3A, 3B or 3C fold, respectively.

The superimposition of a homogeneous flattening strain on a Class 3B fold at an angle θ equal to 0° or 90° modifies its geometry into a Class 3C or 3A fold, respectively (Fig. 5c,d). For a Class 3B fold, the curve through the end points of the isogon rosette is characteristically a rectangular hyperbola of unit axial ratio, $y^2/a^2 - x^2/a^2 = 1$, such that the centre of hyperbola coincides with the common point of intersection of the isogons, with its transverse axis parallel to the fold axial trace (Fig. 5a). As the flattening modifies the Class 3B fold into a Class 3A or Class 3C fold, the rectangular hyperbola transforms into a hyperbola, $y^2/a^2 - x^2/b^2 = 1$ ($a \neq b$), which has two non-orthogonal asymptotes (Fig. 5c,d).

The axial ratio of the non-rectangular hyperbola obtained from the isogon rosette in the Class 3A or Class 3C folds directly gives the strain suffered by the original Class 3B fold during the process of flattening. The maximum principal strain parallels the transverse axis of the hyperbola for Class 3A folds, whereas it parallels the conjugate axis of the hyperbola for Class 3C folds (Fig. 5c,d). In all obliquely flattened Class 3B folds, the major axis of the strain ellipse is inclined with respect to the transverse axis of the hyperbola, i. e.,

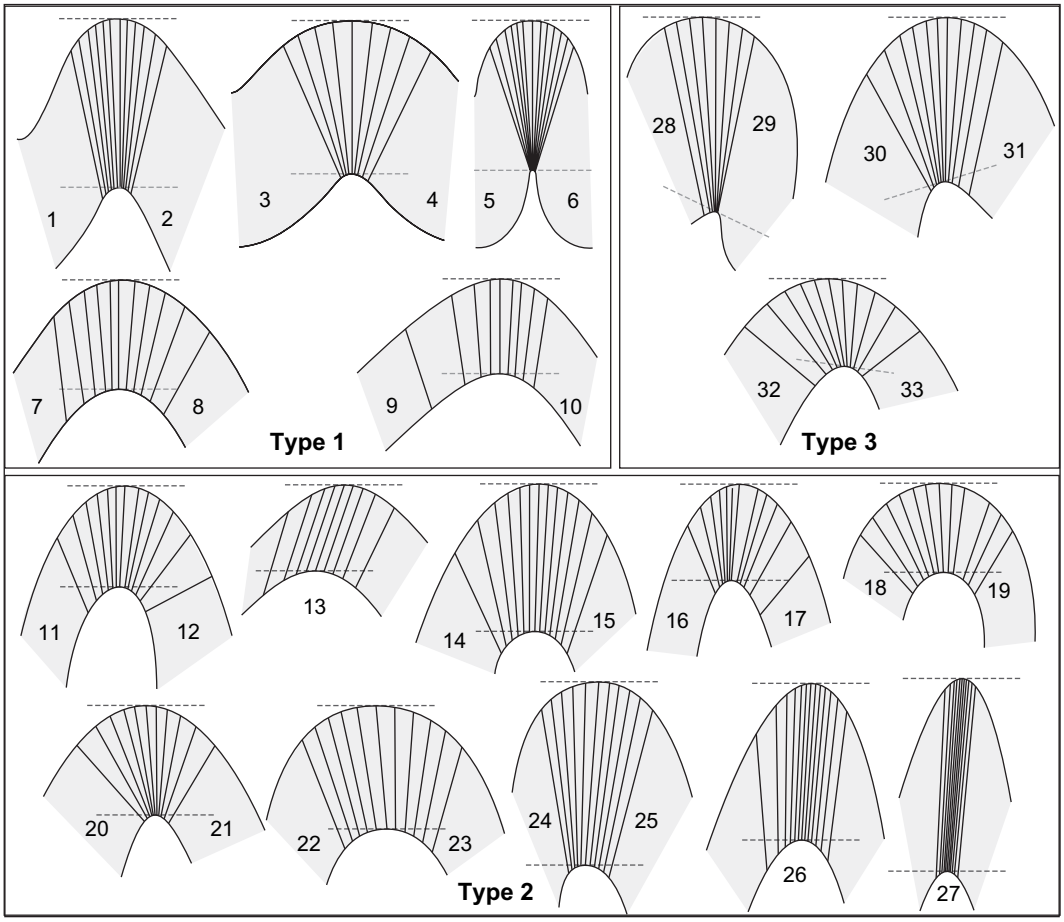

Fig. 4. Examples of the profile sections of Class 1C folds, tested by $t'_\alpha - \alpha$, $\phi - \alpha$ and the "isogon rosette" method (Table 1). Types 1 to 3 are defined in the text.

Table 1
Results obtained using different methods

Fold No. in Fig. 4	Method				
	$t'_\alpha-\alpha$	$\varphi-\alpha$	Isogon rosette		
	R_s	R_s	R_s	θ	RMS
1	2.56	2.85	2.52	0.00	0.016
2	2.27	2.22	2.23	0.00	0.021
3	1.35	1.38	1.36	0.00	0.006
4	1.30	1.33	1.29	0.00	0.007
5	2.08	2.33	2.03	0.00	0.021
6	2.13	2.38	2.11	0.00	0.012
7	2.36	1.96	2.42	0.00	0.003
8	1.54	1.54	1.54	0.00	0.001
9	2.44	1.56	1.86	0.00	0.002
10	2.17	2.44	1.9	0.00	0.005
11	NA	1.91	1.63	−24.50	0.004
12	NA	1.16	1.41	9.38	0.006
13	NA	4.39	3.15	−2.89	0.006
	NA	2.40			
14	NA	1.90	1.65	24.50	0.007
15	NA	2.38	1.88	−12.20	0.010
16	NA	1.88	1.77	−13.40	0.016
17	NA	1.74	1.64	1.42	0.005
18	NA	1.41	1.27	−2.40	0.007
19	NA	1.64	1.65	−2.40	0.006
20	NA	1.42	1.45	6.55	0.097
21	NA	1.17	1.19	−5.10	0.005
22	NA	2.02	1.35	−5.20	0.004
23	NA	1.78	1.53	6.09	0.007
24	NA	2.22	2.21	0.62	0.003
25	NA	2.49	1.80	4.50	0.006
26	NA	3.27	3.17	−2.25	0.007
	NA	4.90			
27	NA	6.7	6.81	−4.40	0.003
	NA	10.5			
28	NA	NA	1.18	19.30	0.003
29	NA	NA	1.36	19.30	0.003
30	NA	NA	1.62	−9.70	0.009
31	NA	NA	1.72	−2.64	0.007
32	NA	NA	1.27	−10.00	0.004
33	NA	NA	1.06	−0.83	0.006

R_s, strain ratio; θ, angle between the maximum principal strain and fold axial trace; RMS, root mean square error in the best-fit ellipse obtained by algebraic fitting. Source for folds: 1 and 2, Hudleston (1973b); 3–6, Dietrich (1969); 7–26, unpublished; 27, Ding and James (1985); 28–33, unpublished. NA, not applicable.

$0^\circ < \theta < 90^\circ$. In practice, the flattening in Class 3 folds can easily be determined using any software, such as the Matlab, which fits the hyperbola through the end points of isogons in the rosette and gives the axial ratio and orientation of the strain ellipse in terms of the axial ratio and orientation of the hyperbola.

6. Use of stretched isogons for fold classification

It has long been accepted that a classification of fold shapes is most appropriately done using differences between the curvatures of the outer and inner arcs of the folded layers (Ramsay, 1967, p. 365; Treagus, 1982; Bastida, 1993). In practice, the curvature difference is expressed by the degree of convergence or divergence of isogons towards fold axial trace. Hence, strongly convergent, moderately convergent, weakly convergent, parallel and divergent isogon patterns characterize Class 1A, Class 1B, Class 1C, Class 2, and Class 3 folds, respectively. In the ''isogon rosette'' method, the nature and orientation of the curve drawn through the end points of the isogons defines the fold geometry (Figs. 2 and 5).

7. Point representation of folds

The problem of representation of a large number of folds on a single $t'_\alpha-\alpha$ or $\phi-\alpha$ plot was first highlighted by Bastida (1993), who proposed a method for representation of a fold limb by the ratio of the slopes of two segments of the curvilinear plot on the $t'_\alpha-\alpha$ graph. This method for point representation of a fold limb, however, requires more measurements and calculations than the $t'_\alpha-\alpha$ method.

Since different fold shapes correspond to different flattening strain ellipses, the parameters R_s and θ can be used for classification and for graphical representation of a fold shape as a point on a $R_s-\theta$ plot (Fig. 6a). The classification scheme assumes that: (i) Class 1C and Class 3C folds form by flattening of Class 1B and Class 3B folds, respectively, at an angle θ equal to 0°, whereas Class 1A and Class 3A folds form by flattening of these folds at an angle θ equal to 90°; and (ii) obliquely flattened Class 1C, or Class 3C folds form by flattening at $0^\circ < \theta < 90^\circ$.

The left and right end points of the horizontal axis on the $R_s-\theta$ plot denote Class 1B and Class 3B folds, respectively (Fig. 6a). ''Similar'' or Class 2 folds plot at the mid-point of the horizontal axis and they correspond to infinitely high amount of flattening of Class 1B or Class 3B folds (Ramsay, 1962). All other points on the horizontal axis represent either Class 1C or Class 3C folds flattened at an angle θ, equal to 0°. Class 1A and Class 3A folds plot on the left- and the right-hand vertical axes, respectively. Obliquely flattened folds plot in upper or lower half of the diagram, depending upon whether the maximum principal strain direction rotates in a clockwise or anticlockwise sense with respect to the fold axial trace, respectively (Fig. 6a). The point representation of all the fold examples in Fig. 4 is shown in Fig. 6a,b.

The concentric arcs, and the radial lines emerging from the two end points of the horizontal axis are, respectively, the curves of constant strain ratio R_s and the lines of constant angle θ (Fig. 6a). The intersection of the R_s curve and the θ lines defines the point that represents a unique fold geometry.

8. Discussion and conclusions

The ''isogon rosette'' method provides the most straightforward technique that allows estimates of two-dimensional strain to be made for flattened folds of Classes 1A, 1C, 3A and 3C, irrespective of the value of angle θ. It only requires drawing a minimum of three isogons and fitting a curve through the end points of isogons in the rosette. The method is free from the errors in identification of precise hinge points, or defining a datum for angular measurements, and importantly does not require any linear or angular measurements, another source of potential error. Amongst all the available

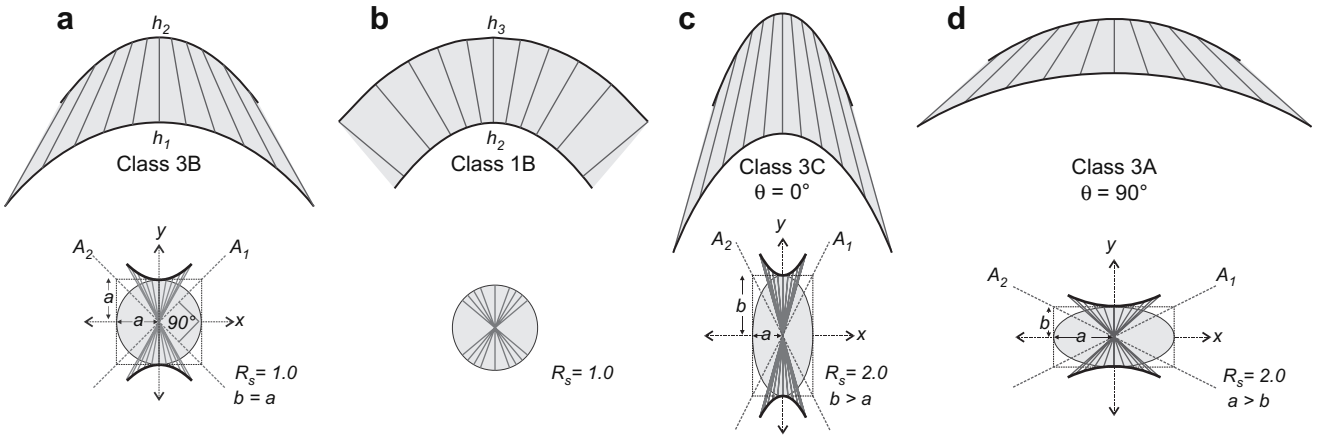

Fig. 5. (a) A Class 3 fold. (b) Class 1B fold obtained by interchanging the outer and inner arcs of the Class 3 fold shown in (a). (c, d) Class 3C and Class 3A folds, respectively. The isogon rosette and the characteristic curve are shown below each fold. The characteristic curve is a rectangular hyperbola, circle, and hyperbolas in (a), (b), (c) and (d), respectively. A_1 and A_2 are asymptotes of hyperbola, and a and b are lengths of the transverse and the conjugate axes of hyperbola. The axial ratio of the hyperbola is given by the aspect ratio of the rectangles. Ellipses inside the rectangles are strain ellipses. R_s, Two-dimensional strain ratio.

methods that can decipher strain in an obliquely flattened fold (Lisle, 1992; Shah and Srivastava, 2006; Srivastava and Shah, 2006), the ''isogon rosette'' method is the most rapid, easy-to-use and accurate. Although the method is related to the method of Lisle (1997), it is conceptually simpler and much more direct.

The ''isogon rosette'' method is, however, not free from assumptions and limitations. For example, it assumes that the flattening follows the buckling, whereas these two processes can operate simultaneously during the folding of rocks. In addition, the method assumes that the shape of the fold prior to flattening conforms to that of a parallel fold irrespective of the fact whether the internal strain inside the parallel fold is accommodated by the tangential longitudinal strain model, the flexural-slip model, or by some combination of these two models (Ramsay, 1967, pp. 391–392; Bastida et al., 2005). For this reason, the method cannot distinguish between flattened tangential longitudinal strain folds and flattened flexural-slip folds.

By using the ''isogon rosette'' method, any fold can be represented by a point whose coordinates are defined by two parameters, R_s and θ. The R_s–θ plot has a much broader scope of applications compared to existing schemes for graphical representation of fold geometry. It is particularly useful for representing the geometry of a large number of folds.

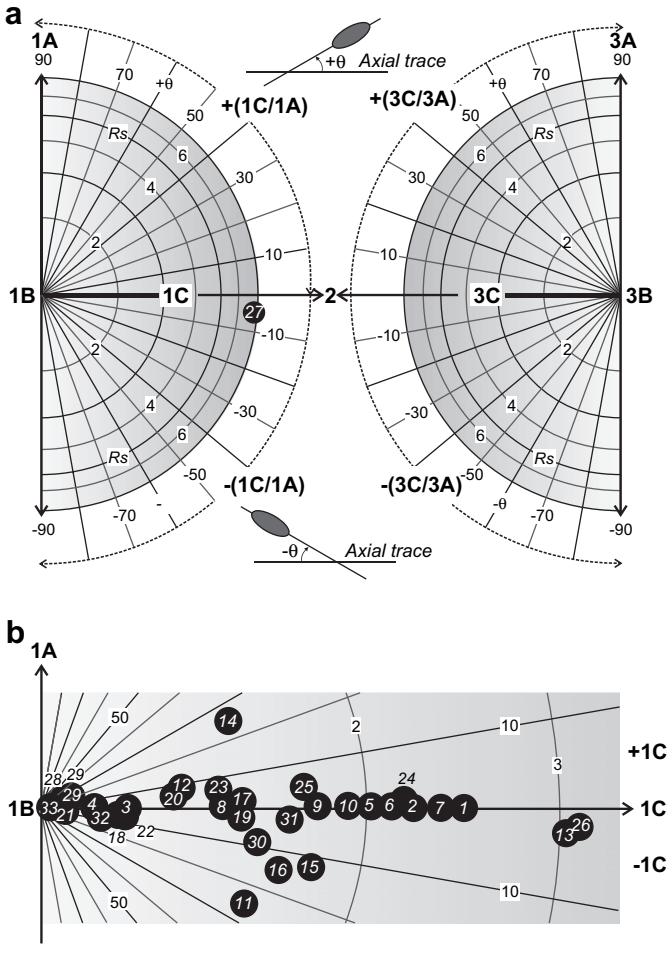

Fig. 6. (a) R_s–θ plot for geometrical classification and point representation of folds (see text for details). (b) Point representation of folds in Fig. 4 in a zoomed portion of the R_s–θ plot shown in (a). White numbers on black dots correspond to fold numbers in Fig. 4. Fold 27 is plotted in (a).

Acknowledgements

This work is funded by the DST Grant of the Government of India. Aditi Pal helped us in testing the method on several examples of folds and Anandroop Ray made the program for searching the best-fit ellipse. Erudite reviews from R.E. Holdsworth, R.J. Lisle and P.W.G. Tanner improved the quality of the paper considerably. Discussions with R.C. Mittal, Nibir Mandal, Ashok Dubey and P. Bhattacharya were helpful during the revision of the manuscript.

References

Bastida, F., 1993. A new method for the geometrical classification of large data sets of folds. Journal of Structural Geology 15, 69–78.

Bastida, F., Aller, J., Bobillo-Ares, N.C., Tomil, N.C., 2005. Fold geometry: a basis for their kinematical analysis. Earth Science Reviews 70, 129–164.

de Sitter, L.U., 1958. Structural Geology. McGraw-Hill, New York, 551 pp.

Dietrich, J.H., 1969. Origin of cleavage in folded rocks. American Journal of Science 267, 155–165.

Ding, P., James, P.R., 1985. Structural evolution of the Harts range arcs and its implication for the development of the Arunta block, Central Australia. Precambrian Research 27, 251–276.

Hudleston, P.J., 1973a. Fold morphology and some geometrical implications of theories of fold development. Tectonophysics 16, 1–46.

Hudleston, P.J., 1973b. The analysis and interpretation of minor folds developed in the Moine rocks of Monar, Scotland. Tectonophysics 17, 89–132.

Lisle, R.J., 1992. Strain estimation from flattened buckle folds: Journal of Structural Geology 14, 369–371.

Lisle, R.J., 1997. A fold classification scheme based on a polar plot of inverse layer thickness. In: Sengupta, S. (Ed.), Evolution of Geological Structures in Micro- to Macro-Scales. Chapman and Hall, London, pp. 323–339.

Naha, K., Halyburton, R., 1977. Structural pattern and strain history of a superposed fold system in the Precambrian of central Rajasthan, India. Precambrian Research 4, 39–84.

Ramberg, H., 1961. Relationship between concentric longitudinal strain and concentric shear strain during folding of homogeneous sheets of rocks. American Journal of Science 259, 382–390.

Ramsay, J.G., 1962. The geometry and mechanics of formation of "similar" type folds. Journal of Geology 70, 309–327.

Ramsay, J.G., 1967. Folding and Fracturing of Rocks. McGraw-Hill, New York, 568 pp.

Ramsay, J.G., 1974. Development of chevron folds. Bulletin of the Geological Society of America 85, 1741–1754.

Shah, J., Srivastava, D.C., 2006. Strain estimation from flattened parallel folds: application of the Wellman method and the Mohr circle. Geological Magazine 143, 243–247.

Srivastava, D.C., Shah, J., 2006. A rapid method for strain estimation from flattened parallel folds. Journal of Structural Geology 28, 1–8.

Srivastava, D.C., Srivastava, P., 1988. Modification of parallel folds by progressive shearing parallel to the axial plane. Tectonophysics 156, 167–173.

Treagus, S.H., 1982. A new isogon-cleavage classification and its application to natural and model fold studies. Geological Journal 17, 49–64.

Wellman, H.W., 1962. A graphical method for analyzing fossil distortion caused by tectonic deformation. Geological Magazine 99, 348–352.

Zagorčev, I.S., 1993. The geometrical classification and distribution of fold types in natural rocks. Journal of Structural Geology 15, 243–251.